Modeling and Measurement of a Tunable Acoustoelastic System

Deborah Fowler[1], Garrett Lopp[2], Dhiraj Bansal[3], Ryan Schultz[4], Matthew Brake[5], Micah Shepherd[6]
[1] Undergraduate Student, University of Massachusetts, Lowell, 01854
[2] Graduate Research Assistant, University of Central Florida, Orlando, FL, 32816
[3] Graduate Student, University of Colorado Boulder, Boulder, CO 80309
[4] Sandia National Laboratories, PO Box 5800-MS0557, Albuquerque, NM, 87123
[5] Assistant Professor, William Marsh Rice University, 6100 Main St, MS 321, Houston, TX 77005
[6] Assistant Research Professor, The Pennsylvania State University, PO Box 30, State College, PA 16804

Acoustoelastic coupling occurs when a hollow structure's in-vacuo mode aligns with an acoustic mode of the internal cavity. The impact of this coupling on the total dynamic response of the structure can be quite severe depending on the similarity of the modal frequencies and shapes. Typically, acoustoelastic coupling is not a design feature, but rather an unintended result that must be remedied as modal tests of structures are often used to correlate or validate finite element models of the uncoupled structure. Here, however, a test structure is intentionally designed such that multiple structural and acoustic modes are well-aligned, resulting in a coupled system that allows for an experimental investigation. First, coupling in the system is identified using a measure termed the magnification factor. Next, the structural-acoustic interaction is measured. Modifications to the system demonstrate the dependency of the coupling on changes in the mode shape and frequency proximity. This includes an investigation of several practical techniques used to decouple the system by altering the internal acoustic cavity, as well as the structure itself. These results show that acoustic absorption material effectively decoupled the structure while structural modifications, in their current form, proved unsuccessful. Readily available acoustic absorptive material was effective in reducing the coupled effects while presumably adding negligible mass or stiffness to the structure.

Keywords: Structural-acoustic interaction, coupled modes, acoustic absorption, acoustic modes, modal testing.

1 Introduction

Acoustoelasticity is the phenomena that describes the coupling between the modal responses of a structure and an enclosed acoustic volume, such as a fluid-filled cavity[1]. Such situations commonly arise in structures within the automotive and aerospace industries[2, 3]. If any modes of the structure and acoustic volume are similar in both shape and frequency, the modal responses can couple and behave similar to a tuned vibration absorber[4]. This coupling leads to an increased number of resonance peaks in the structural response as compared to the in-vacuo structural response. Furthermore, the structural mode shapes will be the same at these additional coupled peaks[5].

If the existence of the acoustoelastic coupling is not known a priori, this can lead to confusion when analyzing the results of a structural modal test used for analytical model correlation. Measurements of the coupled system will exhibit two peaks for each coupled structural-acoustic mode. This can result in the measurement of repeated mode shapes at different frequencies. This pair of modes will have the same structural mode shapes and in- or out-of phase acoustic mode shapes. Consequently, these repeated mode shapes can hamper application of metrics such as the modal assurance criterion (MAC)[6]. Similarly, curve fitters which rely on a modal filter, such as Synthesize Modes and Correlate (SMAC), will have difficulty when using the structural measurements with repeated shapes[7]. Typically, structural dynamics models of structures do not include internal fluid volumes, and therefore the model of a coupled structure will not agree with the results of a modal test. One method of mitigating this issue is by including the fluid loading effects in the analytical model; however, this approach significantly increases model complexity and computational expense. Instead it is desirable if the issue can be mitigated by modifying the test setup. For example, Kim et al. sought to reduce the noise level in a vehicle passenger compartment by decreasing the coupling between certain structural and acoustic modes. They found that by adding structural damping to particular areas of the compartment, coupling was successfully reduced, which resulted in a lower noise level[8].

This work describes the design and testing of an acoustoelastic system, deliberately built to have coupled structure-acoustic mode pairs (Section 2). Using typical modal hammer test methods in conjunction with a roving microphone array, the structure and acoustic mode shapes are obtained in Section 3. In Section 4, the effects of changes to the acoustic and structural components are explored and quantified with a structural frequency response function (FRF).

2 Hardware and Test Design

2.1 Hardware Design

The process for designing a hollow cylindrical shell structure that exhibits acoustoelastic coupling was limited to standard size, off the shelf, aluminum tubing to ease manufacturing and keep cost low. A relatively thick wall was desired, so cylinders with walls ranging from 0.25 inch to 0.5 inch were considered. Next, several finite element models were built with different combinations of radius, wall thickness, and length. An example mesh of a finite element model is shown below. Modes were computed using these models and the low-order ovaling mode frequencies were recorded for comparison with acoustic mode frequencies in Table 1.

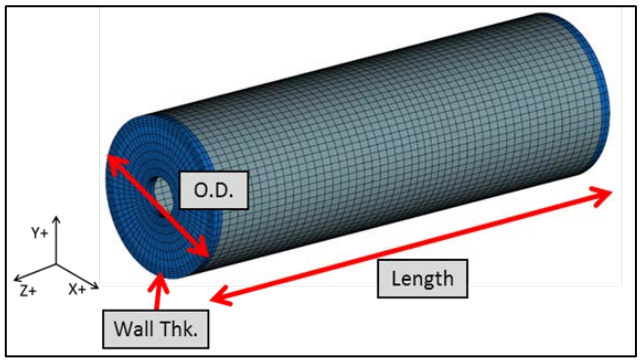

Figure 1. Finite element mesh used to predict the cylinder modes.

The rigid walled acoustic modes were computed analytically for the interior dimensions of each of the candidate cylinder geometries using the equation below[9]:

$$f_{l,m,n} = \frac{c_0}{2}\sqrt{\left(\frac{\alpha_{mn}}{\pi a}\right)^2 + \left(\frac{l}{h}\right)^2}, \quad (1)$$

where c_0 is the acoustic sound speed of the air, a and h are the cylinder inner diameter and length, respectively. The terms l, m, n are the acoustic mode orders in the length, circumference and radius, respectively, and α_{mn} is the n-th zero of the m-order Bessel function of the first kind.

*Table 1. Structure and acoustic mode frequency predictions (in Hz) for different mode orders. * indicates mode outside the analysis range. Modes compatible in shape and frequency are highlighted.*

O.D. [in.]	Wall [in.]	Length [in.]	Shell 2,0	Shell 2,1	Shell 3,0	Shell 3,1	Shell 4,0	Shell 4,1	Acs. 2,0	Acs. 2,1	Acs. 3,0	Acs. 3,1	Acs. 4,0	Acs. 4,1
6	0.50	10	2574	5316	5229	6868	9347	-	2622	2708	3611	3673	4574	4623
6	0.25	12	1525	3777	2512	3605	4530	5176	2384	2449	3282	3330	4158	4196
6	0.50	12	2264	4359	5085	6182	*	*	2622	2682	3611	3654	4574	4608
8	0.25	24	650	1586	1304	1620	2432	2596	1748	1771	2407	2424	3049	3062
8	0.50	20	1177	2292	2728	3196	5046	5381	1873	1903	2579	2601	3267	3284
8	0.50	24	1077	1857	2690	2988	*	*	1873	1894	2579	2594	3267	3279
10	0.25	24	618	1704	873	1348	1559	1780	1380	1408	1900	1921	2407	2424
10	0.50	24	824	1815	1730	2140	3191	3454	1457	1484	2006	2026	2541	2556

Following the calculation of the structure and acoustic mode frequencies for multiple geometries, the geometry that provided the closest matching between at least one pair of structure and acoustic modes (in terms of both shape and frequency) was selected. Using the structure and acoustic modes in Table 1, it was found that an aluminum cylinder with 0.5 inch wall thickness, 8 inch outer diameter and 24 inch length provided good matching at the 2,1 and 3,0 modes. This geometry was used in all subsequent analyses and experiments.

2.2 Experimental Setup

The test specimen was suspended from two bungee cords to approximate a free-free boundary condition, as shown in Figure 2. Both end caps were connected to the cylinder using eight bolts. Figure 2 also shows one end cap with a small hole that enabled a rod holding the microphone array to move and rotate within the structure. Twenty-one uniaxial accelerometers were used to instrument the test specimen, as schematically shown in Figure 3.

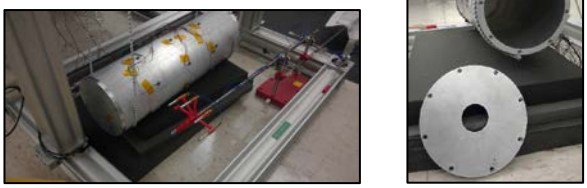

Figure 2. Experimental test setup. Right: Cylinder suspended from soft bungee cords with the accelerometers bonded on the outer surface, and the microphones distributed in an array. Left: Hollow cylinder with end cap removed.

Figure 4 shows the axial locations traversed by the array of microphones used to capture the acoustic modes of interest of the internal air cavity as well as the angular location of each microphone taken from the +X axis. A 3-D printed microphone holder held the microphones fixed with a separation angle of 45 degrees between each microphone. Two measurements were taken at each of the seven axial locations within the cavity (i.e. with the microphone holder positioned at 0 degree and 180 degrees). This set of 14 measurement locations captured the acoustic mode shapes of the cavity with acceptable resolution for the low-order acoustic modes of interest. This approach allowed for many more pressure measurement locations than the number of available microphones and is akin to the traditional roving accelerometer technique used in modal testing.

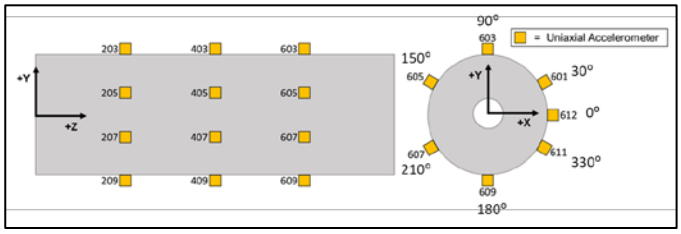

Figure 3. Accelerometer measurement locations.

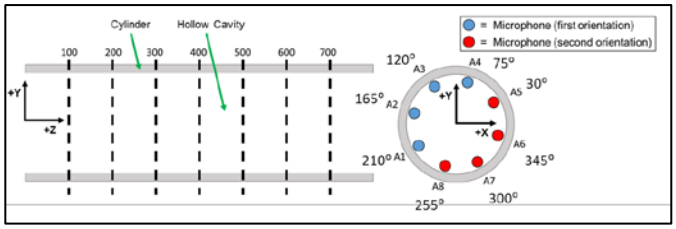

Figure 4. Microphone measurement locations within the cylinder cavity.

3 Identification and Measurements of Acoustoelastic Coupling

This section introduces methods for both identifying and measuring the acoustoelastic coupling in the system. A modal impact hammer excited both the structure and the coupled acoustic response of the internal cavity. A method is introduced to identify the frequency ranges where the system seems to exhibit acoustoelastic coupling when both microphone and accelerometer data is available. Measurements of the structural and acoustic mode shapes are shown to demonstrate which modes are active at coupled regions of the FRF.

3.1 Coupling Identification

Coupling is identified through a simultaneous analysis of acoustic measurements and structural measurements. Figure 5 shows both the acoustic FRF from microphone A3 located at axial station 600 as well as the average structural FRF from all the accelerometer measurements. Averaging the FRF magnitudes of all accelerometers is a simple method of condensing the data. It can be seen that more acoustic modes are excited than structural modes for this system. Three are several acoustic modes which align in frequency with the structural modes, however strong coupling effects were not observed at each of

these mode pairs. These additional acoustic peaks indicate that, although coupling does exist, it is not large enough to appreciably effect the structural response. In order to quickly identify when an appreciable amount of coupling exists to affect the structural response, a quantitative measure termed the magnification factor MF was defined as:

$$MF = \left| \frac{H_{Ac}}{H_{St,RMS}} \right| \quad (2)$$

in which H_{Ac} is the acoustic FRF at a point inside the cavity and $H_{St,RMS}$ is the RMS value of the average structural FRF across the entire frequency range of interest. Figure 5 also shows the MF at every frequency line and the sharp peaks indicate large coupling. In this frequency range of interest, three frequency bands exhibit large coupling: 1700-2000 Hz, 2550-2700 Hz, and 2900-3000 Hz.

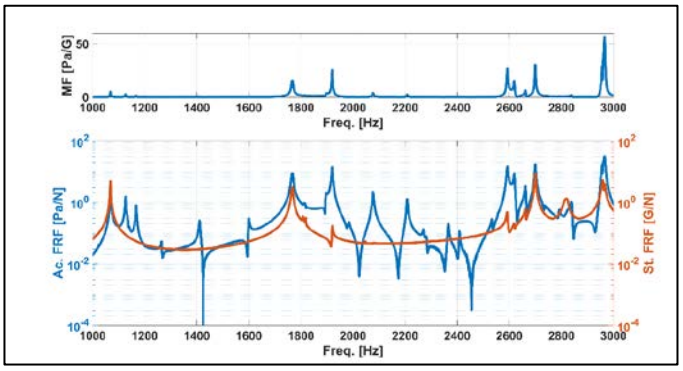

Figure 5. Top: Magnification factor as a function of frequency. Bottom: Acoustic FRF for a single microphone location (left axis) and structural FRF averaged over all locations (right axis).

3.2 Coupled Mode Shapes

This section outlines the procedure used to measure the coupled structural-acoustic modes. The cylindrical test article showed symmetry requiring two hammer impacts at locations 603 and 605 (60° apart) to separate the repeated roots. An initial test provided the acceleration responses with the microphones removed from the cavity. To obtain the modal parameter estimates (frequencies, damping values, and mode shapes)**,** the Polymax curve fitting routine built-in with the LMS Test. Lab software was used[10]. The results presented here focus on the 1700-2000 Hz frequency range where the first set of coupled modes exist, as indicated in Figure 5. Figure 6 shows the structural drive-point FRF at location 603 over this range as well as the structural mode shapes shown with the hollow surface elements. The first peak near 1790 Hz is the location of two repeated (2, 1) ovaling modes where the anti-node of the first mode was orientated with the +Y-axis of the cylinder and the second mode showed a 45° rotation. The second peak near 1820 Hz is two repeated bending modes but did not exhibit coupling with any acoustic modes. The third peak near 1920 Hz is the location of the coupled (2, 1) ovaling modes.

One challenge in measuring the coupled acoustic mode shapes was that the microphones were not acoustically transparent. As a result, the microphones added a perturbation to the acoustic cavity at each measurement location. Since the microphones were roved throughout the cavity, the boundary conditions are slightly different for each measurement. For example, there was a slight frequency shift in the modes near 1920 Hz as the microphone array moved along the axial direction of the cavity. Such a shift required modal parameter estimations at each microphone location to obtain the local mode shapes which were then stitched together to produce the full cavity mode shape. Similar to the structural mode shapes, the acoustic mode shapes also showed repeated roots due to the symmetry of the internal cylindrical cavity. Figure 6 also shows the acoustic mode shapes for each mode of interest as filled volumes. Outward deflections indicate high pressure while inward deflections indicate low pressure. Furthermore, the first set of modes near 1790 Hz show that both the structural and acoustic modes oscillate in-phase, while the coupled pair near 1920 Hz show out-of-phase motion. These results are consistent with the findings in a previous numerical study that showed the lower frequency mode of a coupled pair exhibited this in-phase motion while the higher frequency mode exhibited out-of-phase motion[5]. This result also makes sense when comparing this coupling behavior to a vibration absorber where the two coupled masses show in-phase motion at the lower modal frequency, and out-of-phase motion at the higher modal frequency[4].

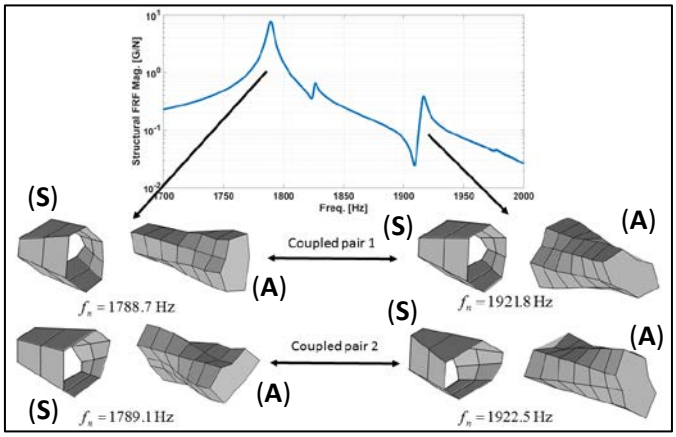

Figure 6. Structural drive-point FRF with the associated coupled structural-acoustic modes shown. Hollow surfaces represent structural displacement mode shapes (S), and filled volumes represent acoustic pressure mode shapes (A) (positive and negative deflections correspond to positive and negative pressures).

4 Coupling Mitigation Strategies

This section details the strategies employed to mitigate the acoustoelastic coupling and is separated into two approach methodologies: Acoustic cavity modifications and structural modifications. Although there are three frequency ranges that exhibit coupling, this investigation focuses on the 1700-2000 Hz frequency range for brevity. Similar results were seen for the coupled modes in the other frequency ranges.

4.1 Acoustic Modifications: Boundary Condition Modification with a Partition

As an initial attempt to disrupt the acoustic mode shapes and to reduce coupling, Figure 7 shows a cardboard partition inserted into the cavity and suspended with a rod to avoid contact with the structure. The partition is included to alter the boundary conditions on the acoustic cavity and was placed at three different axial locations to examine the effect of location on response. With the partition placed at the center, termed Location 1, which coincided with the axial node line of the acoustic pressure shape, there was minimal effect on the coupling. As the partition travelled closer to the end of the cylinder where the pressure magnitudes increased, the coupling decreased, though did not completely disappear. This result is surprising as the expectation was that locating the partition closer to the edge would approximate an empty cylinder with no partition. The reason for this discrepancy may be that the partition was not fully rigid, and that there were air gaps around the periphery. A more rigorous implementation of the boundary condition modification may be needed before drawing further conclusions.

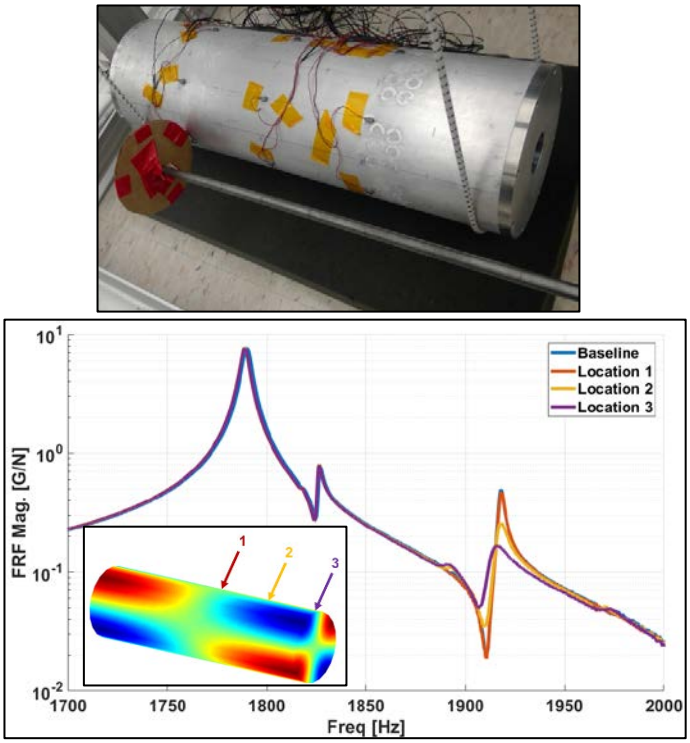

Figure 7. Inclusion of cardboard partition within cylinder cavity. Left: Cardboard disk partition connected to a rod to suspend it inside the cavity. Right: Structural FRF magnitude with the partition at three axial locations, compared against the baseline FRF.

4.2 Acoustic Modifications: Acoustic Damping Modification with Absorptive Material

As an alternative to disrupting the acoustic mode shapes, a second approach to modifying the acoustic behavior involved the introduction of acoustic damping to remove the acoustic energy from the system in a similar manner to Schultz et al.[4] by inserting foam blocks into the cavity. Two different methods were utilized to insert the foam: Figure 8 shows the first method with foam wrapped around the rod suspended in the cavity such that it was not contacting the structure. The effects of this added acoustic damping on the structural FRF are shown in Figure 8. The objective was to incrementally add layers of foam and study the effect of the amount of foam on the response, but even at the smallest amount, 27% fill, the coupled mode was effectively removed. Increasing layers of foam did not have a strong effect on the FRF, though a shift in the main mode frequency is observed, which is consistent with the vibration absorber model for the coupled system used in Schultz et al.[4].

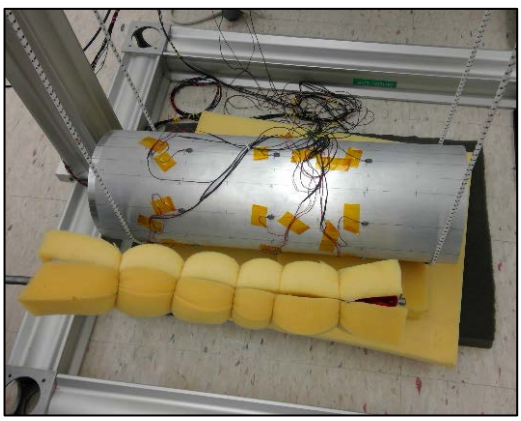

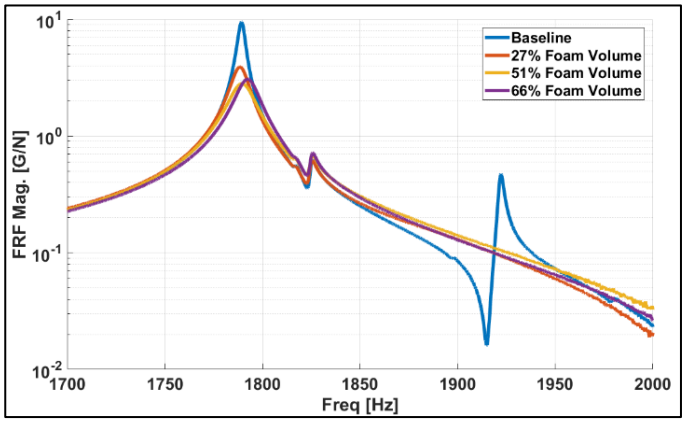

Figure 8. Inclusion of foam as an acoustic damper inside the cylinder cavity. Left: Foam wrapped around a rod and suspended in the cavity. Left: Effect of the foam on the structural FRF.

The second method involved incrementally inserting two inch foam cubes into the cavity. Figure 9 shows the foam cubes located within the cavity. The FRF shows that for the same volume of foam, the foam cubes provided more acoustic damping and offers better reduction in coupling as compared with the foam wrapped around a rod. One reason may be that wrapping the foam around the rod caused some compression in the foam, reducing the acoustic absorption potential. Although using foam cubes does require some contact with the structure, the mass-loading effect of the foam on the structure was negligible. Furthermore, inclusion of the foam eliminated the coupling from the 1.8 kHz and 2.7 kHz structural peaks with approximately 23% and 5% of the cavity filled with foam, respectively. The structural peaks at these frequencies also exhibited small shifts in frequency and decreases in damping after increasing the volume of foam past critical threshold.

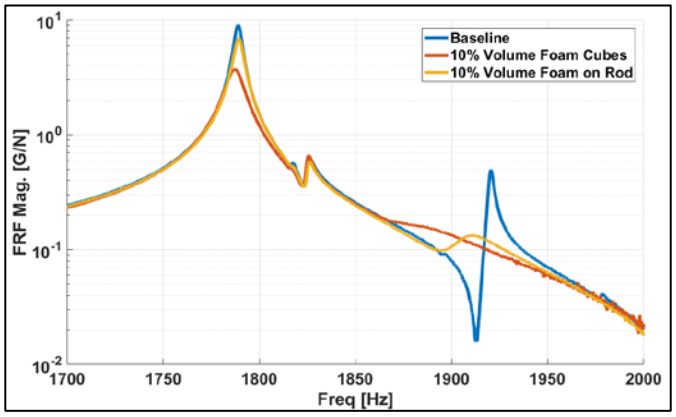

Figure 9. Comparison between the two foam approaches: Foam placed within the cavity as cubes (contacting), and foam wrapped around rod suspended in cavity (non-contacting).

These results qualitatively agree with the response of a simple two degree-of-freedom system shown in Figure 10[4]. Here, the main mass is the structure and the second mass is the air. When the second mass is in-tune to the mode frequency of the main mass, there is a split in the peak. When there is some frequency mistuning, the shift if frequency away from the main peak is less dramatic. Similarly, if damping is added to the second mass the second peak amplitude begins to decrease and effectively disappears with higher damping.

Other possibilities of introducing acoustic absorption while adding negligible mass to the system included randomly distributing common household paper towels within the cavity. Figure 11 shows the paper towels randomly distributed in the cavity and the corresponding effect on the FRF. Paper towels provided similar acoustic damping and decoupling as the foam cubes. The nature of the absorption provided by the paper towels is not understood; it is unlikely they provide a significant change in boundary condition and the lack the extensive, tortuous pore structure of open cell foam.

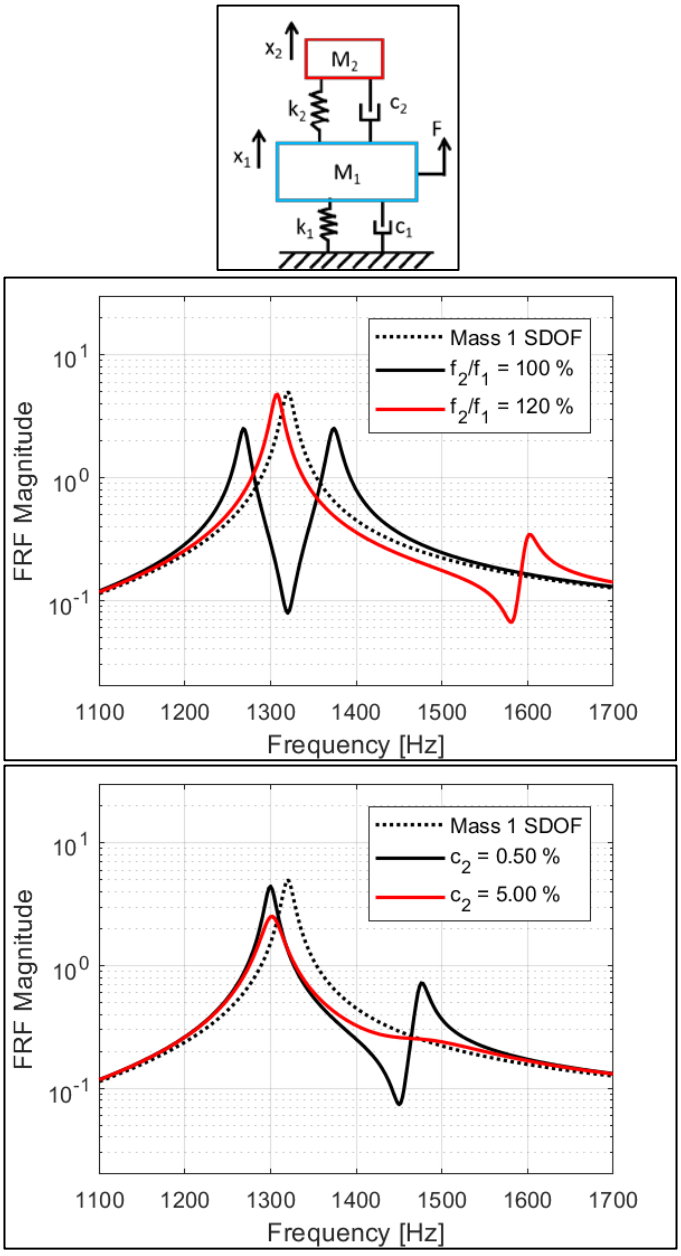

Figure 10. Two DOF system (left), effect of frequency mistuning on coupled system response (center) and effect of Mass 2 damping on coupled system response (right).

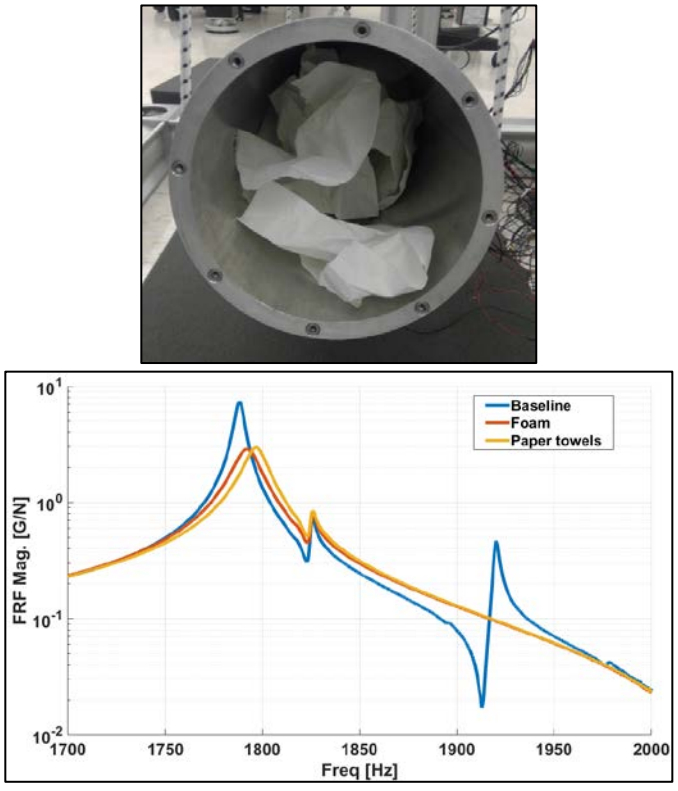

Figure 11. Randomly distributing house-hold paper towels within the cavity as an acoustic absorber, Left. Right: Effect on the FRF and compared against the baseline, empty cavity and the cavity with foam cubes.

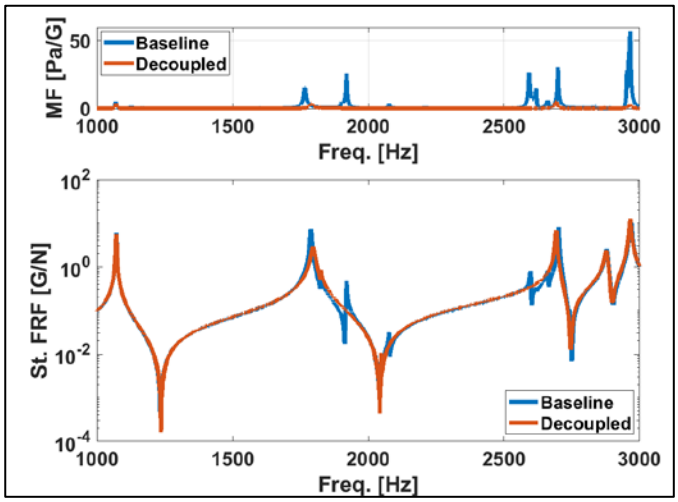

Figure 12. Comparison of the decoupled and coupled structural FRFs and magnification factor with the decoupled response obtained by including paper towels within the cavity.

Figure 12 shows the decoupling of the full frequency range tested using the paper towels. The extra peaks associated with the coupled acoustic modes are no longer present in the structural FRF, clearly indicating the effectiveness of this approach. As a second measure of the effectiveness of this approach, the sharp peaks present in the magnification factor corresponding with the coupled modes show a significant reduction.

4.3 Structural Modifications: Added Mass

In some cases, the internal cavity of the system may not be accessible and the previously described acoustic modifications will not be

available. Instead the structure would need to be modified to affect the acoustoelastic coupling. This was explored by adding mass to the structure, thereby shifting the structural component mode frequencies. Figure 13 shows steel nuts that provided the mass-loading on the structure. Bonding clusters of these masses at the antinodes of the (2, 1) structural mode with even spacing every 45° around the structure ensured adequate mass-loading for both repeated roots. Figure 13 shows that the largest applied mass induced more than a 150 Hz frequency shift for the structural peak. A much smaller frequency shift occurred for the coupled peak with a corresponding reduction in the peak amplitude; the coupling, however, was not fully removed. Also, the added mass caused a second acoustic mode near 1895 Hz to begin coupling with the structure, an unintended and seemingly unpredictable consequence caused by the shifting of the structural frequencies. Although not entirely effective in its current form, this method should be further explored by adding significantly more mass to induce more dramatic structural frequency shifts and mode shape perturbations. Structural dynamic modification techniques could then be used to computationally remove the added mass and calculate the structural response[11]. Methods to alter the stiffness of the structure were also considered and attempted, but no effective solution was found in the range of stiffnesses considered.

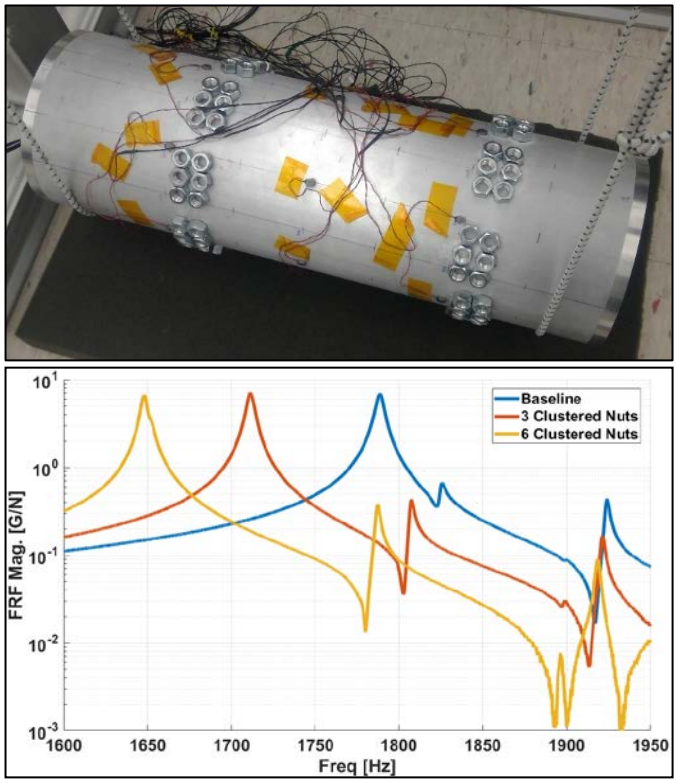

Figure 13. Mass added at anti-node locations of the target mode to shift structural frequencies, Left. Right: Effect of added mass on the FRF.

5 Conclusions and Future Work

This paper explored the phenomena of acoustoelastic coupling and developed ways of identifying, measuring, and mitigating the coupling effects observed in the structural response. Typical hammer impact tests on a hollow aluminum cylinder allowed for measurements of the coupled system FRFs. Development of a quantitative measure, termed the magnification factor, led to quick identification of the modes exhibiting large coupling. Extracting displacement mode shapes of the structure and pressure mode shapes for the acoustic cavity revealed in-phase motion for the lower frequency coupled pair, and out-of-phase motion for the higher frequency pair.

Several mitigation strategies were investigated to remove the effects of the acoustoelastic coupling on the structural FRF. When the acoustic cavity is accessible, acoustic modifications showed the most promise in removing the coupling behavior. Selectively locating flexible partitions within the acoustic chamber did reduce, but not satisfactorily mitigate, the coupling behavior. However, including acoustic absorption material within the cavity successfully decoupled the structural response and typical house-hold paper towels proved to be an effective mitigation method. For situations where the cavity may be inaccessible, the structural modifications employed so far have been unsuccessful.

Although some of the mitigation strategies outlined above provided a decoupled structural response, methods for determining whether this is the true in-vacuo response still require investigation. One method may be to include the structural-acoustic interaction in the analytical, coupled system model and investigate how changing damping in the air component model changes structural response and how that new response compares against the structure-only model response.

References

1. Dowell, E. H., Gorman, G. F., Smith, D. A., "Acoustoelasticity: General theory, acoustic natural modes and forced response to sinusoidal excitation, including comparisons with experiment," Journal of Sound and Vibration, Vol. 52, No. 4, pp. 519-542, 1977.
2. Jha, S. K., "Characteristics and sources of noise and vibration and their control in motor cars," Journal of Sound and Vibration, Vol. 47, No. 6, pp. 543-558, 1976.
3. Davis, R. B., Joji, S. S., Parks, R. A., Brown, A. M., "Acoustic-structure interaction in rocket engines: Validation testing," Conference Proceedings of the IMAC-XXVII, Orlando, FL, 2009.
4. Schultz, R., Pacini, B.,"Mitigation of structural-acoustic mode coupling in a modal test of a hollow structure," Conference Proceedings of the Society for Experimental Mechanics Series: Rotating Machinery, Hybrid Test Methods, Vibro-Acoustics & Laser Vibrometry, Vol. 8, pp. 71-84, 2017.
5. Pacini, B., Tipton, G., "Structural-acoustic mode coupling in a bolted aluminum cylinder," Conference Proceedings of the Society for Experimental Mechanics Series: Topics in Modal Analysis & Testing, Vol. 10, pp. 393-401, 2016.
6. Allemang, R., "The modal assurance criterion: Twenty years of use and abuse," Sound and Vibration, August 2003.
7. Mayes, R. L., Klenke, S. E., "The SMAC modal parameter extraction package," Conference Proceedings of the IMAC-XVII, 1999.
8. Kim, S. H., Lee, J. M., Sung, M. H., "Structural-acoustic modal coupling analysis and application to noise reduction in a vehicle passenger compartment," Journal of Sound and Vibration, Vol. 225, No. 5, pp. 989-999, 1999.
9. Blackstock, D. T., "Fundamentals of physical acoustics," Wiley, 2000.
10. Peeters, B., Van der Auweraer, H., Guillaume, P., Leuridan, J., "The PolyMAX frequency-domain method: A new standard for modal parameter estimation?," Shock and Vibration, Vol. 11, No. 3-4, pp. 395-409, 2004.
11. Avitabile, P. "Twenty years of structural dynamic modification-a review," Sound and Vibration, January 2003.

The author can be reached at: rschult@sandia.gov.